Experimental Control of a PEM Water Electrolyzer: Investigation of Renewable Energy Source Framework

Meziane Ait Ziane, Michel Zasadzinski, Ayat-Allah Bouramdane, Elodie Pahon and Hugues Rafaralahy

Abstract—This paper is dedicated to the control of hydrogen production with an experimental proton exchange membrane water electrolyzer in the context of renewable energy sources. Two control laws, iP and PI controllers have been evaluated under several scenarii including RES variations. A discussion of the performances of the controllers allows to formulate several open issues for the control of PEMWEs in a renewable energy context.

I. Introduction

Achieving carbon neutrality by 2050 requires a significant effort to reduce greenhouse gas emissions, which is a real challenge. One key solution to this challenge is to use hydrogen as an energy carrier and make hydrogen production as environmentally friendly as possible. Hydrogen production using Water Electrolyzers (WE) powered by Renewable Energy Sources (RES) such as wind turbines and photovoltaic panels is consistent with this solution. The most appropriate water electrolyser technology in the context of RES is the Proton Exchange Membrane Water Electrolyzer (PEMWE), thanks to its ability to operate in the presence of variations in the energy source and their high current density about 2 A/cm², in contrast to the alkaline water electrolyzer.

A PEMWE works at low voltage in comparison to power supplied, so mostly a DC/DC buck converter is used to ensure that the PEMWE operates accordingly to the desired current [1], [2]. In such case, the system to be controlled becomes the whole PEMWE + DC/DC converter. Using the well know Farday's law the control of hydrogen production is based on the PEMWE current.

In the literature, PEMWEs have been modeled as an electrical circuit: as a simple resistor in [3], [4] and as an RC circuit in [5], [6]. A more complex model based on thermal, electrical and chemical relationships can be found in [7], [8]. However, from an experimental point of view, it is difficult to use these models due to the difficulty of accurately determining their physical parameters.

The PID controller is the most employed control strategy for current control of PEMWE due to its simplicity of the

This work was not supported by any organization

M. Ait Ziane is with Université de Lorraine, GREEN, F-54000 Nancy, France. meziane.ait-ziane@univ-lorraine.fr

M. Zasadzinski and Hugues Rafaralahy are with Research Center for Automatic Control of Nancy (CRAN), UMR CNRS 7039, Université de Lorraine, F-54000 Nancy, France michel.zasadzinski@univ-lorraine.fr, hugues.rafaralahy@univ-lorraine.fr

Ayat-Allah Bouramdane is with LERMA lab, International University of Rabat, Morocco ayatallah.bouramdane@uir.ac.ma

Elodie Pahon is with Université Marie et Louis Pasteur, UTBM, CNRS, Institut FEMTO-ST, FCLAB, F-90000 Belfort France elodie.pahon@utbm.fr

tuning parameters [4], [9], [10], [11]. It should be noticed that these PID have been not designed on an experimental test bench and have not been analysed in realistic RES context, i.e. by taking into account the variations of the supplied energy. A control law based on an identified model is proposed in [12] and validated in simulation by taking into account variations in the supplied RES.

In this article, hydrogen production is investigated on a PEMWE test bench (see Fig. 1) in a RES framework. Obtaining a PEMWE model that describes actual system behavior is a difficult task, so the control of yhis PEMWE is made without using any model. Two control strategies corresponding to this approach without model, model-free control [13], [14] and PID control, are retained in this paper. The aim of this paper is to rely on control law performances analysis to formulate open and realistic issues for the control of PEMWEs within a renewable energy context.

This paper is structured as follows. The experimental test bench is described in Section II. The designs of *i*P and PI controllers are given in Section III. Section IV is dedicated to the experimental results: the 1st considered scenario with desired current changes is presented in Section IV-A, the 2nd treated scenario with both changes for desired current and supplied voltage of RES is given in Section IV-B and the 3rd scenario is dedicated to the robustness against strong supplied voltage RES variations in Section IV-C. Section V deals, on the one hand, with the analysis of closed-loop performances and, on the other hand, with the open questions generated from this analysis with regard to PEMWE control in RES framework. The conclusion is given in Section VI.

II. EXPERIMENTAL TEST BENCH DESCRIPTION

The test bench used in this paper is composed of a PEMWE coupled with a DC/DC converter as shown in Fig. 1.



Fig. 1: Experimental test bench

Table I gives the specifications of the PEMWE stack used in this paper.

TABLE I: PEMWE stack technical specifications

Parameters	Values	Units
Rated power	400	W
Cell number N_c	3	
Max current	50	A
Active area	50	cm ²

The DC/DC converter is a Stacked Interleaved Buck Converter (SIBC) (see [15] for more explanations on SIBC design) and its diagram is given in Fig. 2 where $L_p=L_s=426\times 10^{-6}\,\mathrm{H},~R_{\ell_p}=R_{\ell_s}=0.06\,\Omega,~C_p=10^{-4}\,\mathrm{F}$ and $C_s=10^{-5}\,\mathrm{F}.$

The acquisition of the PEMWE stack current I and voltage V are performed using dSPACE dS1104 board with a sampling time $T_s=0.001\,\mathrm{s}$. This dSPACE board allows to send the control signal u to the Pulse Width Modulation (PWM) generator Matlab/Simulink block to drive the power switches of the SIBC.

An interface board converts 0-5 V PWM signals to 0-15 V signals required by the SEMIKRON driver boards SKHI 22. The frequency switching of the PWM is 20 kHz, i.e. $T_{\rm pwm} = 5 \times 10^{-5}$ s. The whole system is supplied by a device called EA-PS 980-100 where the voltage V_{RES} is generated by dSPACE. The voltage V_{RES} emulates the variations of the power provided by RES like wind or PV.

The opposite control of the two circuits of the SIBC (the primary one with index p and the secondary with index s) is achieved by two pairs of insulated-gate bipolar transistors (\mathcal{T}_1 , \mathcal{T}_4) during the duty cycle $(1-D)T_{\mathrm{pwm}}$ and (\mathcal{T}_2 , \mathcal{T}_3) during the duty cycle DT_{pwm} where D is a percentage of the period $T_{\mathrm{pwm}} = 5 \times 10^{-5} \, \mathrm{s}$ of PWM.

III. DESIGN OF THE iP AND PI CONTROLLERS

The control objective is to ensure a desired hydrogen flow rate. The hydrogen production \dot{m}_{H_2} by the PEMWE is linked to the applied current to the PEMWE via the following relation

$$\dot{m}_{H_2} = \frac{N_c I}{2F} \eta_{H_2} \tag{1}$$

where N_c is the number of cells in the stack, I is the current applied to the PEMWE (see Fig. 2) and η_{H_2} is the Faraday's efficiency coefficient taken as 0.97 in our application. So based on relation (1) and in a control point of view, the desired hydrogen production can be expressed through a desired current trajectory called I^* .

Since the behavior of the entire system shown in Fig. 2 is nonlinear due to the interaction between electrical, thermal and chemical phenomena, it is very difficult to obtain a model that accurately describes the system, which is beyond the scope of this document. That is the reason why the two control laws proposed below are not based on an analytical model, but are directly tuned on the process.

The 1^{st} controller design used in this paper is model-free control or iP controller proposed in [13], [14]. This approach

is based on an ultra-local model defined by

$$y^{(\mu)}(t) = \mathcal{F}(t) + \rho u(t) \tag{2}$$

where

- y and u are the output and the control variables, respectively,
- the order of output derivation y is μ , where $\mu = 1$ in this paper,
- ρ is a user-tuned parameter,
- the function F contains the unknown part of the system and is estimated according to the input and output of the system.

In the case of $\mu = 1$, the estimate of \mathcal{F} is given by [16]:

$$\hat{\mathcal{F}}(t) = \frac{-3!}{T^3} \int_{t-T}^t (T - 2t)y(t) + \rho t(T - t)u(t)dt$$
 (3)

where T>0 is small and [t-T;t] refers to the sliding windows of the integration interval. The closed-loop control in the case of the iP controller with $\mu=1$ is defined by:

$$u(t) = \frac{1}{\rho} \left(-\hat{\mathcal{F}}(t) + \dot{y}^{\star}(t) + k_p e(t) \right) \tag{4}$$

where

- y* is the desired trajectory determined using a secondorder dynamics filter as in [17],
- $e = y^* y$ is the tracking error,
- $k_p = 250$ is the tuning gain of the proportional part of the controller,
- $\rho = 35000$.

The $2^{\rm nd}$ controller design is a PI controller corresponding to controller $C_1(s)$ in [18]. Note that $C_1(s)$ was designed in [18] by using the same test bench as in this paper. Since the derivative action does not appear in the control law given by (4), the derivative action in $C_1(s)$ is not taken into account. The PI control law is given by

$$u(t) = K_p \left(1 + \frac{1}{T_i s} \right) (y^* - y) \tag{5}$$

where $s \in \mathbb{C}$ is the Laplace variable and

- $K_p = 0.001$,
- $T_i = 0.00205$.

In our application, y^* and y stand to I^* and I, respectively.

IV. EXPERIMENTAL RESULTS

In this section, the control laws given in (4) and (5) are applied on the test bench illustrated in Fig. 1. Three scenarii are considered:

- 1st scenario is dedicated to the responses to desired current I^* changes where the supplied voltage of RES $V_{RES} = 40 \, \mathrm{V}$ is constant (see Section IV-A),
- 2nd scenario considers the responses to desired current
 I* changes where the supplied voltage of RES, V_{RES},
 is not constant: the variations of V_{RES} emulate the
 variations provided by the wind turbine (see Section
 IV-B).
- $3^{\rm rd}$ scenario studies the robustness of the two control laws against strong variations of supplied voltage V_{RES} (see Section IV-C).

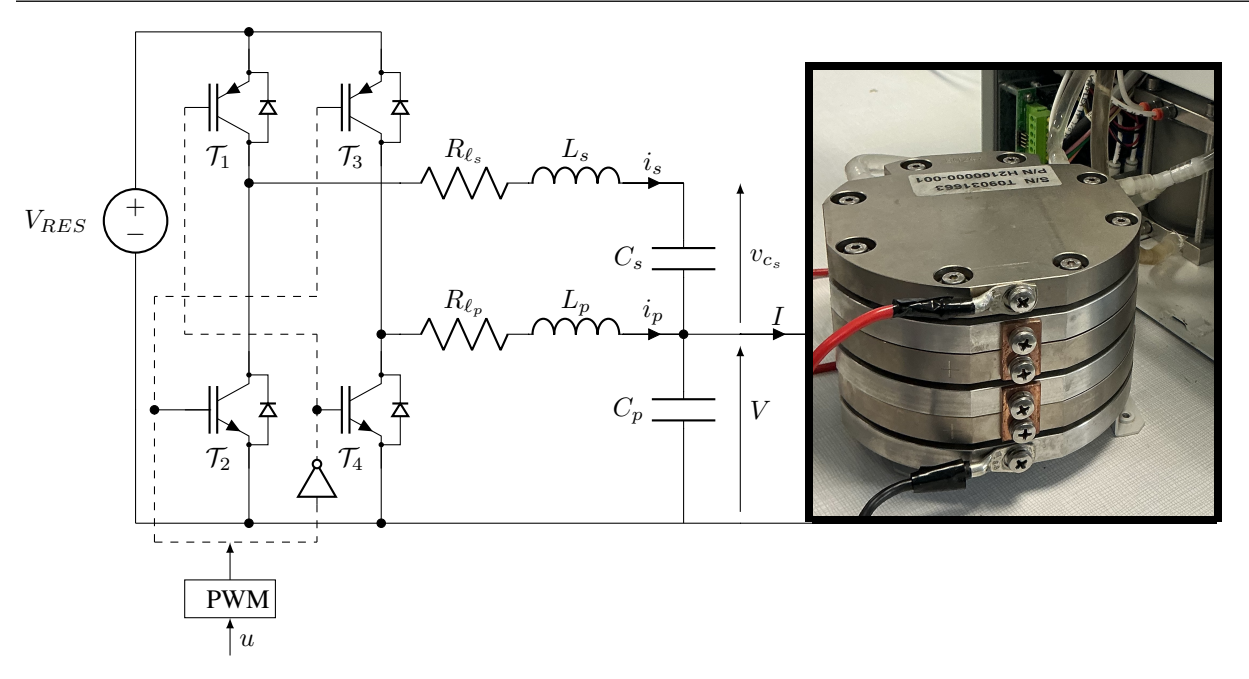


Fig. 2: Stacked interleaved DC-DC buck converter with pulse width modulation and PEM water electrolyzer

A. Variations of the desired hydrogen production

In this section, variations in the desired hydrogen production are applied and represented by changes in I^* , as shown in Fig. 3. For better see the behavior of the iP and PI control laws, two zooms are made in Fig. 4 and Fig. 5.

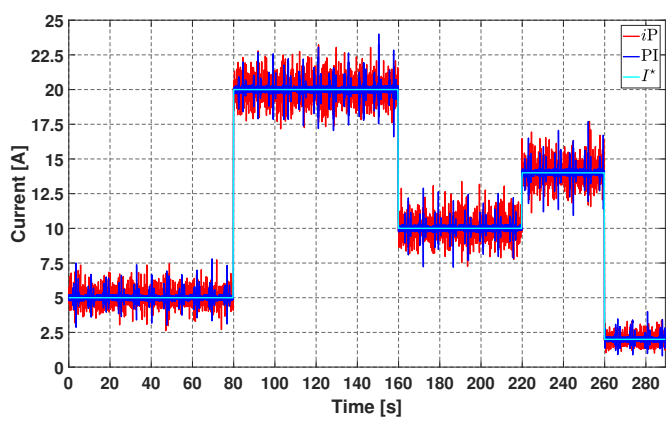


Fig. 3: Changes of operating current steps

Both iP and PI controllers ensure the tracking of the desired current I^* in the event of upward or downward changes without overshoot. In Fig. 4 and Fig. 5, the settling time of the three signals, i.e. reference I^* and current I generated by both the iP and PI controllers are less than $0.1 \, \mathrm{s}$. However, it can be seen that the stabilization time obtained with the iP closed loop is slightly faster than that with the PI closed loop. We therefore conclude that both controllers work well for this scenario.

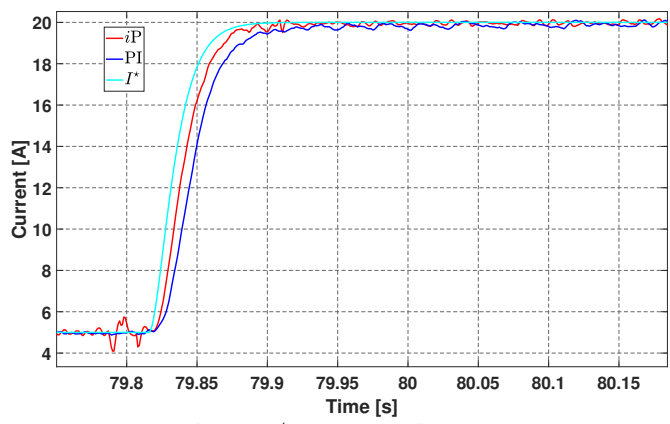


Fig. 4: 1st zoom on Figure 3

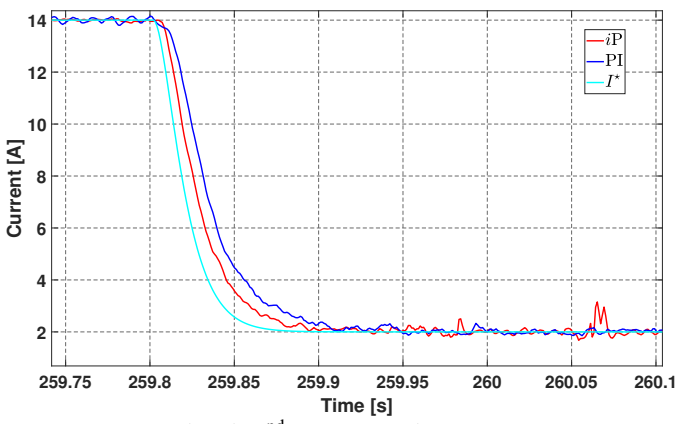


Fig. 5: 2nd zoom on Figure 3

B. Variations of both hydrogen production and supplied V_{RES} by wind turbine

The emulated supplied voltage V_{RES} by wind turbine is given in Fig. 6 with the variations of the desired hydrogen

production that are represented by changes in I^* , as shown in Fig. 7.

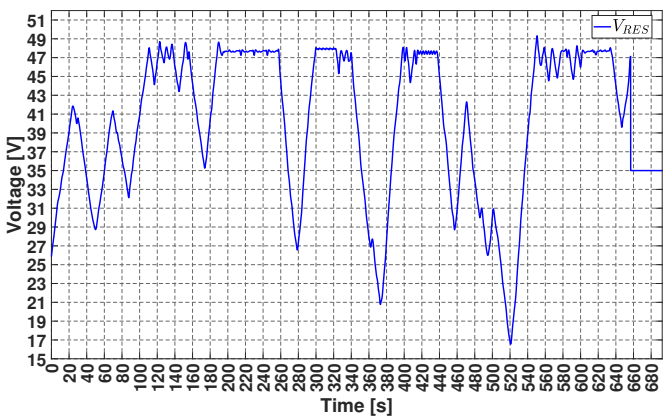


Fig. 6: Variations of $V_{RES}(t)$ supplied by wind turbine

To highlight the obtained closed-loop behaviors with both iP and PI control laws, three zooms are made in Fig. 7, Fig. 8 and Fig. 9.

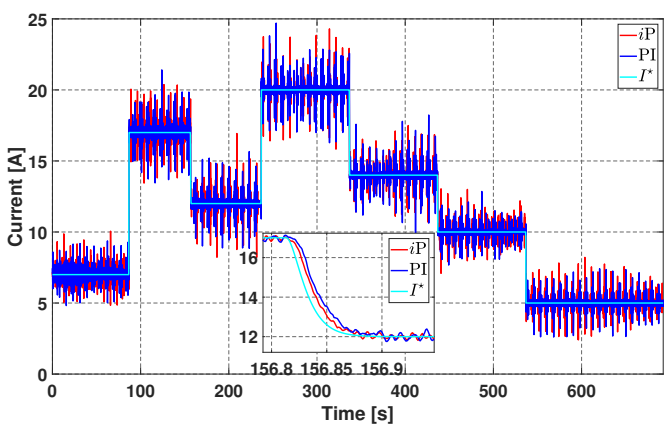


Fig. 7: PEMWE current I(t) responses due to variations of both hydrogen production and V_{RES} voltage supplied by wind turbine

The whole duration of this experiment is about $11.5 \, \mathrm{min}$. The large variations of V_{RES} in Fig. 6 have almost no effects on the current I responses generated by $i\mathrm{P}$ and PI controllers as shown in Fig. 7. To illustrate this point, the large variations in V_{RES} around $280 \, \mathrm{s}$, $370 \, \mathrm{s}$ and $520 \, \mathrm{s}$ in Fig. 6 do not significantly affect the steady-state behavior of the closed-loop current responses I in the time intervals $[240 \, \mathrm{s} \ 340 \, \mathrm{s}]$, $[340 \, \mathrm{s} \ 440 \, \mathrm{s}]$ and $[440 \, \mathrm{s} \ 540 \, \mathrm{s}]$ in Fig. 7, respectively.

The variations in voltage V_{RES} supplied by a wind turbine feeding the SIBC and PEMWE can be considered as an uncertaintiy in the system that the iP and PI controllers should take into account. These variations in V_{RES} reflect the actual behavior of the voltage supplied by a renewable energy source. Several changes on the desired current I^* when V_{RES} is changing are made in order to evaluate the closed-loop with iP and PI controllers.

Fig. 7, Fig. 8 and Fig. 9 zoom in on two desired current I^* changes for the overall scenario considered. The iP and PI

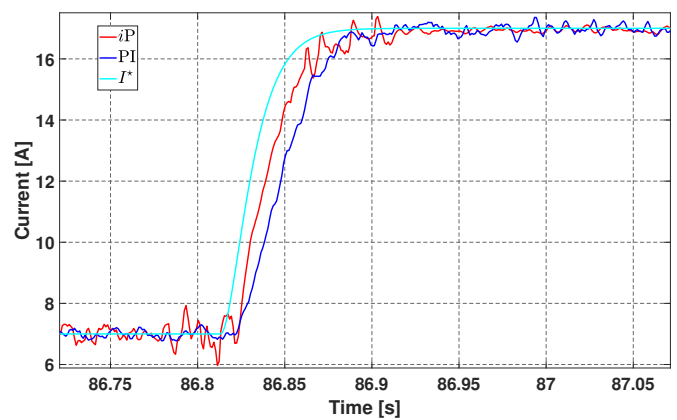


Fig. 8: 1st zoom on Figure 7

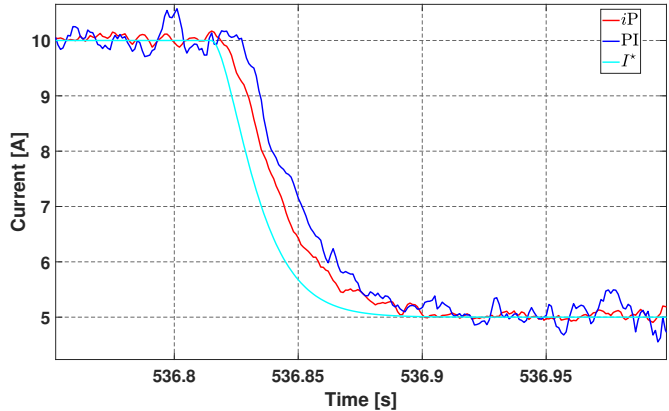


Fig. 9: 2nd zoom on Figure 7

controllers guarantee that the desired current I^* is followed without any noticeable overshoot. The same settling time as in Section IV-A is obtained for all three signals, and it can be seen that the response of the current I with the iP controller is marginally faster than with the PI controller. However, both controllers ensure a good tracking of the desired trajectory under V_{RES} variations.

C. Robustness to strong variations of RES supplied energy

The results obtained in Section IV-B have shown that the impact of V_{RES} variations in Fig. 6 is minor on the regulated current I with both controllers iP and PI. This confirms the robustness of the two control laws against V_{RES} variations. In this section, strong variations in V_{RES} are considered to assess the ability of the iP and PI controllers in maintaining the desired hydrogen production. These variations in V_{RES} are less representative of the RES than the variations considered in Section IV-B. However, strong variations of V_{RES} can be regarded as realistic in an isolated micro-grid situation where voltage variations are abrupt. The duration of this scenario is about 7.7 min with variation of $V_{RES} \in [24 \, \mathrm{V} \ 37 \, \mathrm{V}]$ as shown in Fig. 10.

The current I is regulated at $15\,\mathrm{A}$ and the response of this current under strong V_{RES} variations with both $i\mathrm{P}$ and PI controllers are shown in Fig. 11. At first look, Fig. 11 shows that closed-loop behavior with the PI controller exhibits

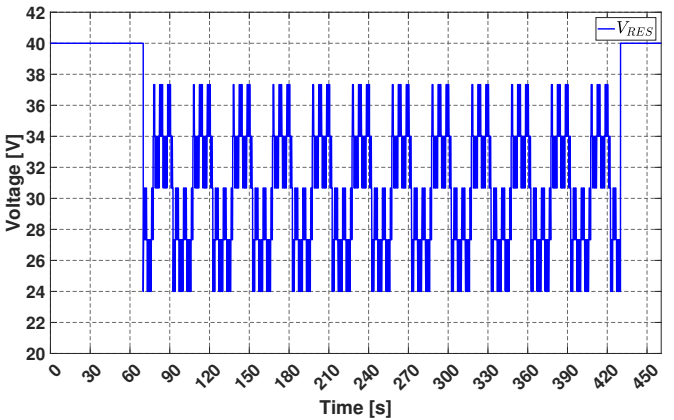


Fig. 10: Strong variations of supplied RES voltage V_{RES}

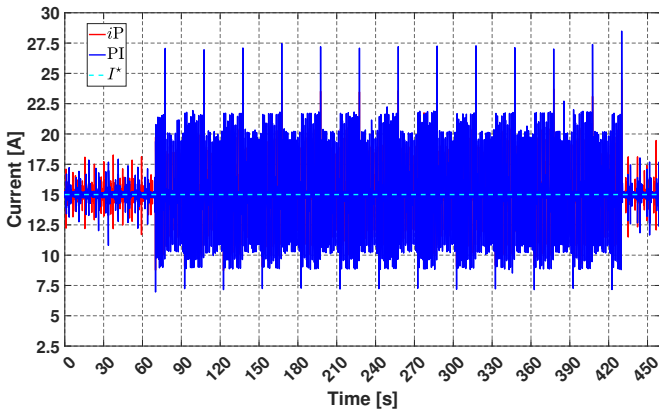


Fig. 11: PEMWE current I(t) responses due to variations of supplied RES voltage V_{RES} in Figure 10

higher fluctuations than with the *i*P controller. Zooms in Fig. 12 and Fig. 13 confirm this fact.

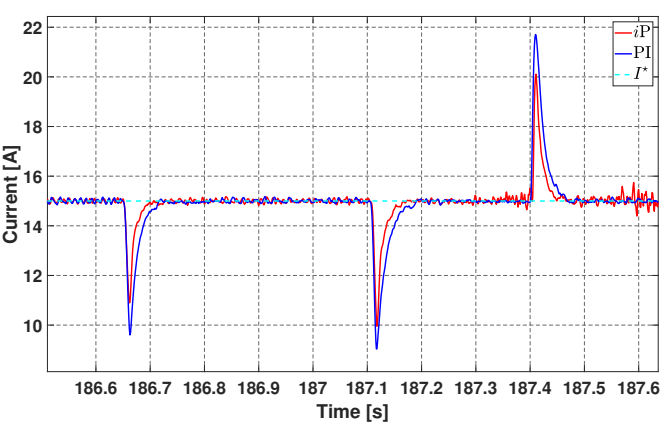


Fig. 12: 1st zoom on Figure 11

Unlike in the responses given in Section IV-B, zooms in Fig. 12 and Fig. 13 show that the impact of the variations of V_{RES} on the regulated current I is plainly visible. The rejection of these variations in transient behavior is better for the iP controller that the PI controller (see the peaks in Fig. 12 and Fig. 13). For the two control laws, these variations are asymptotically rejected. As in Sections IV-A and IV-B, the settling time with iP controller is slightly faster than the

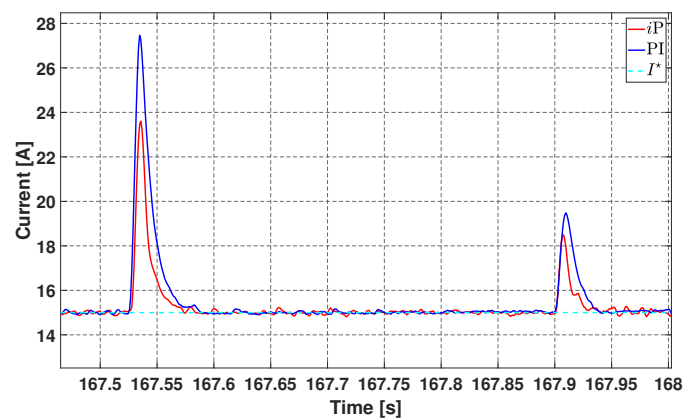


Fig. 13: 2nd zoom on Figure 11

one with PI controller.

The control input u for both iP and PI controllers is shown in Fig. 14. If we compare Fig. 10 and Fig. 14, we can see that the two control laws react quickly to the abrupt changes of V_{RES} without peaks in the transient behavior (see the zoom in Fig. 14).

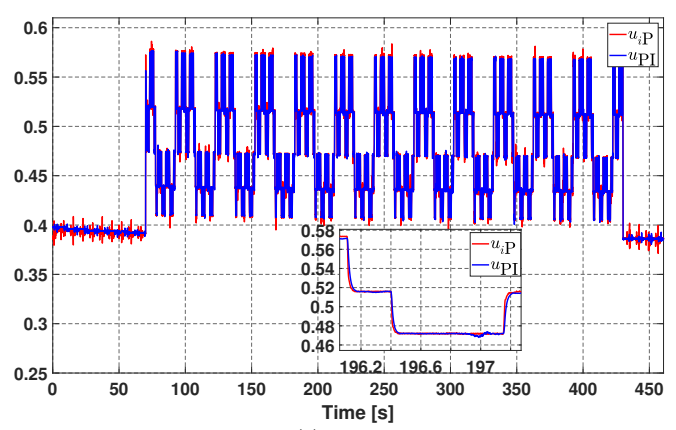


Fig. 14: Control signal u(t) responses due to variations of supplied RES voltage V_{RES} in Figure 10

V. DISCUSSION

This discussion is based from the obtained results. The objective is to propose some open questions related to the control of PEMWE under RES variations.

(1) Summary of experimental results:

The 1st scenario considered in this paper shows that the tracking of the desired current I^* is achieved in 0.1 s with iP and PI controllers.

In the $2^{\rm nd}$ scenario, realistic variations in the voltage V_{RES} supplied by a wind turbine have no significant effect on the regulated current I, i.e. the controllers iP and PI maintain the current at the desired value despite these realistic variations.

In the $3^{\rm rd}$ scenario, strong variations of V_{RES} are considered, these variations are asymptotically rejected by both $i{\rm P}$ and PI controllers.

(2) Settling time of controlled PEMWE versus realistic variations of V_{RES} :

Since variations in V_{RES} supplied by the wind turbine have no significant effect on the regulated current I, the following questions can be raised.

- a) The voltage variations V_{RES} supplied by the RES has a slower dynamic than the dynamic of the used PEMWE. Could we find ourselves in a situation where the voltage dynamic V_{RES} is faster than that of the PEMWE in a real application?
- b) The PEMWE studied in this article consists of 3 cells. Do increasing the number of cells have an impact on the dynamics of the PEMWE current and on what scale?
- c) With strong V_{RES} variations, we have significant peaks which can accelerate the degradation of the PEMWE. What is the probability of encountering such variations in V_{RES} in a real application? The controller design is based on trajectory tracking, so is a design based on disturbance rejection more appropriate for this application? With this alternative design, will peaks be much more attenuated?

(3) RES power:

In this paper, the context of RES is considered as voltage variations. In the case where power supplied by a RES system is considered, the following questions are raised.

- a) Variations in RES power do not allow the desired current to be maintained where the power supplied is not sufficient. In this situation, can we say that we have a reference I^* generation problem?
- b) This case also generates many situations where the control input u will be saturated, so what method should be used for desaturation?

VI. CONCLUSION

The control of the hydrogen production is treated in this paper by addressing the challenges of the RES framework. The control of hydrogen production consists on the control of PEMWE current. Two controllers *i*P and PI where their design is made in model-free and are evaluated under variations of the voltage provided by RES.

Both iP and PI controllers ensure a quick tracking of the desired hydrogen production and guarantee the maintain of the desired current under V_{RES} variations with a slight advantage for the iP controller. These results have raised several open questions for the control of PEMWEs in a renewable energy context.

REFERENCES

- [1] V. Guida, D. Guilbert, G. Vitale, and B. Douine, "Design and realization of a stacked interleaved DC-DC step-down converter for PEM water electrolysis with improved current control," *Fuel Cells*, vol. 20, pp. 307–315, 2020.
- [2] B. Yodwong, D. Guilbert, W. Kaewmanee, M. Phattanasak, M. Hinaje, and G. Vitale, "Improved sliding mode-based controller of a high voltage ratio DC-DC converter for electrolyzers supplied by renewable energy," *IEEE Trans. Industrial Electronics*, vol. 71, pp. 8831–8840, 2024

- [3] F. Alonge, S. Collura, F. D'Ippolito, D. Guilbert, M. Luna, and G. Vitale, "Design of a robust controller for DC/DC converterelectrolyzer systems supplied by μWECSs subject to highly fluctuating wind speed," *Control Engineering Practice*, vol. 98, p. ID 104383, 2020
- [4] M. Şahin, H. Okumuş, and M. Aydemiri, "Implementation of an electrolysis system with DC/DC synchronous buck converter," *Int. J.* of Hydrogen Energy, vol. 39, pp. 6802–6812, 2014.
- [5] M. Agredano-Torres, M. Zhang, L. Söder, and Q. Xu, "Decentralized dynamic power sharing control for frequency regulation using hybrid hydrogen electrolyzer systems," *IEEE Trans. Sustainable Energy*, vol. 15, pp. 1847–1858, 2024.
- [6] Á.. Hernández-Gómez, V. Ramirez, and D. Guilbert, "Investigation of PEM electrolyzer modeling: electrical domain, efficiency, and specific energy consumption," *Int. J. of Hydrogen Energy*, vol. 45, pp. 14625– 14639, 2020.
- [7] R. Keller, E. Rauls, M. Hehemann, M. Müller, and M. Carmo, "An adaptive model-based feedforward temperature control of a 100 kW PEM electrolyzer," *Control Engineering Practice*, vol. 120, p. ID 104992, 2022.
- [8] P. Olivier, C. Bourasseau, and B. Bouamama, "Low-temperature electrolysis system modelling: a review," *Renewable and Sustainable Energy Reviews*, vol. 78, pp. 280–300, 2017.
- [9] M. Şahin, "A photovoltaic powered electrolysis converter system with maximum power point tracking control," *Int. J. of Hydrogen Energy*, vol. 45, pp. 9293–9304, 2020.
- [10] M. Koundi, H. El Fadil, Z. El Idrissi, A. Lassioui, A. Intidam, T. Bouanou, S. Nady, and A. Rachid, "Investigation of hydrogen production system-based PEM EL: PEM EL modeling, DC/DC power converter, and controller design approaches," *Clean Technologies*, vol. 5, pp. 531–568, 2023.
- [11] A. Antoniou, C. Celis, R. Mas, A. Berastain, N. Xiros, G. Papageorgiou, A. Maimaris, and T. Wang, "Effective thermal-electric control system for hydrogen production based on renewable solar energy," *Int. J. of Hydrogen Energy*, vol. 53, pp. 173–183, 2024.
- [12] M. Zasadzinski, M. Ait Ziane, and R. Rafaralahy, "Robust control of PEM electrolyzer in a renewable energy context," in *Proc. IEEE Conf. Decision & Control*, (Milano, Italy), 2024.
- [13] M. Fliess and C. Join, "Model-free control," Int. J. Control, vol. 86, pp. 2228–2252, 2013.
- [14] M. Fliess and C. Join, "An alternative to proportional-integral and proportional-integral-derivative regulators: Intelligent proportionalderivative regulators," *Int. J. Robust & Nonlinear Contr.*, vol. 32, pp. 9512–9524, 2022.
- [15] J. Wibben and R. Harjanii, "A high-efficiency DC-DC converter using 2 nH integrated inductors," *IEEE J. of Solid-State Circuits*, vol. 43, pp. 844–854, 2008.
- [16] M. Mboup, C. Join, and M. Fliess, "Numerical differentiation with annihilators in noisy environment," *Numerical Algorithms*, vol. 50, pp. 439–467, 2009.
- [17] M. Ait Ziane, M. Péra, C. Join, M. Benne, J. Chabriat, N. Yousfi Steiner, and C. Damour, "On-line implementation of model free controller for oxygen stoichiometry and pressure difference control of polymer electrolyte fuel cell," *Int. J. of Hydrogen Energy*, vol. 47, pp. 38311–38326, 2022.
- [18] R. Maamouri, D. Guilbert, M. Zasadzinski, and H. Rafaralahy, "Proton exchange membrane water electrolysis: modeling for hydrogen flow rate control," *Int. J. of Hydrogen Energy*, vol. 46, pp. 7676–7700, 2021.